

# Glutathione depletion activates the yeast vacuolar transient receptor potential channel, Yvc1p, by reversible glutathionylation of specific cysteines

Avinash Chandel, Krishna K. Das, and Anand K. Bachhawat\*

Department of Biological Sciences, Indian Institute of Science Education and Research (IISER), Mohali 140306, Punjab, India

**ABSTRACT** Glutathione depletion and calcium influx into the cytoplasm are two hallmarks of apoptosis. We have been investigating how glutathione depletion leads to apoptosis in yeast. We show here that glutathione depletion in yeast leads to the activation of two cytoplasmically inward-facing channels: the plasma membrane, Cch1p, and the vacuolar calcium channel, Yvc1p. Deletion of these channels partially rescues cells from glutathione depletion-induced cell death. Subsequent investigations on the Yvc1p channel, a homologue of the mammalian TRP channels, revealed that the channel is activated by glutathionylation. Yvc1p has nine cysteine residues, of which eight are located in the cytoplasmic regions and one on the transmembrane domain. We show that three of these cysteines, Cys-17, Cys-79, and Cys-191, are specifically glutathionylated. Mutation of these cysteines to alanine leads to a loss in glutathionylation and a concomitant loss in calcium channel activity. We further investigated the mechanism of glutathionylation and demonstrate a role for the yeast glutathione S-transferase Gtt1p in glutathionylation. Yvc1p is also deglutathionylated, and this was found to be mediated by the yeast thioredoxin, Trx2p. A model for redox activation and deactivation of the yeast Yvc1p channel is presented.

**Monitoring Editor**  
Charles Boone  
University of Toronto

Received: May 6, 2016  
Revised: Sep 14, 2016  
Accepted: Sep 27, 2016

## INTRODUCTION

Two important hallmarks of cells that undergo apoptosis are glutathione depletion (Franco *et al.*, 2008) and a rapid increase in cytosolic calcium (Orrenius *et al.*, 2003). Glutathione depletion can occur through efflux, through consumption and oxidation by metals and reactive oxygen species (ROS), through the reduction in biosynthe-

sis, or through cytosolic glutathione degradation. The second recognized feature in apoptotic cells is a rapid and transient influx of calcium into the cytosol and subsequently into the mitochondria (Giorgi *et al.*, 2008). The concentration of calcium in the cytosol is around 100 nM. Extracellular calcium levels are much higher (1.5 mM), and in specific organelles like the endoplasmic reticulum and vacuole, the free intracellular calcium concentration can be between 300 and 30  $\mu$ M, respectively (Dunn *et al.*, 1994; Bootman *et al.*, 2001; Clapham, 2007). During apoptosis, depending on the stimulus, the cytosolic calcium levels can rise either through influx from the extracellular  $Ca^{2+}$  pool or through efflux from the intracellular stores, leading to a transient increase in calcium levels up to 1  $\mu$ M concentrations (Bootman *et al.*, 2001). These two events, glutathione depletion and calcium influx, have reciprocal interactions in the cell (Brookes *et al.*, 2004). Calcium levels can affect ROS and glutathione through multiple mechanisms, while ROS generated in different compartments by different means can in turn strongly affect calcium levels through different mechanisms. Thus there appears to be a well-regulated but complex interplay of these different molecules that is still not entirely understood (Puigipóns *et al.*, 2015; Tajeddine, 2016).

This article was published online ahead of print in MBoc in Press (<http://www.molbiolcell.org/cgi/doi/10.1091/mbc.E16-05-0281>) on October 5, 2016.

\*Address correspondence to: Anand K. Bachhawat ([anand@iisermohali.ac.in](mailto:anand@iisermohali.ac.in), [anand.bachhawat@gmail.com](mailto:anand.bachhawat@gmail.com)).

Abbreviations used: GRX, glutaredoxin; GSH, reduced glutathione; GSSG, oxidized glutathione; GST, glutathione S-transferase; HRP, horseradish peroxidase; IAM, iodoacetamide; IgG, immunoglobulin G; NEM, N-ethylmaleimide; PBS, phosphate-buffered saline; PI, propidium iodide; PMSF, phenylmethylsulfonyl fluoride; RLU, relative luminescence unit; ROS, reactive oxygen species; SD, synthetic defined; TRP, transient receptor potential; TRX, thioredoxin; WT, wild type; YPD, yeast extract, peptone, and dextrose.

© 2016 Chandel *et al.* This article is distributed by The American Society for Cell Biology under license from the author(s). Two months after publication it is available to the public under an Attribution–Noncommercial–Share Alike 3.0 Unported Creative Commons License (<http://creativecommons.org/licenses/by-nc-sa/3.0>).

"ASCB®" "The American Society for Cell Biology®," and "Molecular Biology of the Cell®" are registered trademarks of The American Society for Cell Biology.

Glutathione depletion and oxidative stress are also known regulators of apoptosis in yeast (Weinberger *et al.*, 2003; Carmona-Gutierrez *et al.*, 2010). We have been interested in investigating how glutathione depletion triggers apoptosis in the yeast *Saccharomyces cerevisiae*. In a previous study, we have shown that, in glutathione-deficient yeast cells, apoptosis could be significantly enhanced merely by overexpressing ChaC1, a cytosolic enzyme for glutathione degradation (Kumar *et al.*, 2012). Glutathione depletion, which is normally thought to act through an increase in ROS, can also function by a ROS-independent mechanism (Han *et al.*, 2008; Franco and Cidlowski, 2009), and it was of importance to determine the immediate downstream events of glutathione depletion in yeast. As a starting point for investigating the early events resulting from glutathione depletion, we first sought to look into the possible interplay between calcium homeostasis and glutathione depletion.

In the yeast *S. cerevisiae*, two calcium channels are thought to be primarily responsible for the flux of calcium into the cytoplasm. The first is the plasma membrane high-affinity calcium transport system comprising Cch1p/Mid1p/Ecm7p; and the second is Yvc1p (Cunningham, 2011), located on the vacuole, the primary intracellular store of calcium in yeast (Dunn *et al.*, 1994). The Cch1p channel shows similarity to the human L-type calcium channels, while Yvc1p is a mechanosensitive channel that shows similarity to the mammalian transient receptor potential (TRP) channels (Palmer *et al.*, 2001; Denis and Cyert, 2002). The Cch1p and Yvc1p channels are both redox sensitive and osmosensitive (Matsumoto *et al.*, 2002; Popa *et al.*, 2010). However, the exact mechanisms by which these channels are regulated is not known.

In the present study, we investigated the effects of intracellular glutathione depletion, and we demonstrate that glutathione depletion-induced apoptosis in yeast is calcium dependent and can be rescued by deletions in the two channels that pump calcium into the cytoplasm, Cch1p and Yvc1p. We demonstrate that these transporters are activated during glutathione depletion due to changes in the intracellular redox state of the cell. Mutational analysis revealed that Yvc1p is glutathionylated at specific cysteine residues, resulting in channel activation and calcium influx into the cytoplasm. Further, we demonstrate that the glutathionylation occurs enzymatically through the yeast glutathione S-transferase Gtt1p and that this mechanism is reversible, with the deglutathionylation being mediated by thioredoxin, Trx2p.

## RESULTS

### Glutathione depletion leads to an enhanced calcium sensitivity in *S. cerevisiae*

Glutathione depletion can cause both ROS-dependent responses and non-ROS-dependent responses (Franco and Cidlowski, 2009). Because oxidative stress has previously been shown to lead to an influx of calcium into the cytoplasm of yeast (Popa *et al.*, 2010), the possibility existed that glutathione depletion was also leading to an oxidative stress and through this ROS-dependent pathway was giving rise to increased intracellular calcium. To carry out some preliminary investigations in this direction, we examined the sensitivity of yeast depleted of glutathione to calcium stress using *S. cerevisiae gsh1Δ* cells. *S. cerevisiae gsh1Δ* cells bear a deletion in the glutathione biosynthetic gene (*GSH1*) and are glutathione auxotrophs. These strains were grown on different concentrations of extracellular glutathione and exposed to high concentrations of calcium (Figure 1A). We observed that, at low concentrations of glutathione, the cells displayed a greater calcium sensitivity, while at higher concentrations of supplemented glutathione, the cells were less sensitive to

calcium, suggesting that glutathione depletion might in fact be causing increased calcium levels intracellularly.

Glutathione is a known chelator of several heavy metals such as lead, arsenic, cadmium, and zinc. There are no reports of chelation of calcium by glutathione. We examined whether the above observations might be a consequence of glutathione chelation of calcium. To investigate this, we carried out binding assays with calcium, but although we could detect binding of glutathione with zinc, as has been reported (Chekmeneva *et al.*, 2008), we could not find any detectable binding of glutathione to calcium, suggesting that the effects that were being observed were not a consequence of chelation of calcium by glutathione (unpublished data).

To examine the calcium sensitivity of glutathione-depleted cells more rigorously, we carried out growth experiments in the presence of the intracellular calcium chelator BAPTA-AM. BAPTA-AM is a membrane-permeable compound that is capable of chelating intracellular calcium; thus BAPTA-AM can control free cytoplasmic Ca<sup>2+</sup> at low levels (Li *et al.*, 2011). *S. cerevisiae gsh1Δ* cells in the absence of glutathione can grow for a few generations by using the intracellular glutathione pool before the cells enter growth stasis finally leading to cell death (Sharma *et al.*, 2000). We observed that, in the presence of the calcium chelator BAPTA-AM, cell growth was prolonged and cell death due to glutathione depletion was significantly rescued (Figure 1B), although no discernible changes in intracellular glutathione were observed (unpublished data). Apoptosis assays further confirmed that BAPTA-AM significantly rescued the apoptosis due to glutathione depletion (Figure 1, C–E).

### Glutathione depletion causes an increase in cytoplasmic calcium levels: correlation with the redox milieu

Because intracellular calcium chelation by BAPTA-AM rescued the glutathione depletion-induced cell death, it suggested that the cytoplasmic influx of calcium might be occurring, as has been observed during oxidative stress (Ermak and Davies, 2002; Popa *et al.*, 2010). To examine whether glutathione depletion led to a similar calcium influx, we carried out calcium measurements using the aequorin assay. We observed that the *S. cerevisiae gsh1Δ* cells that were shifted from high-glutathione medium to glutathione-free medium showed a gradual increase in calcium levels. We also compared this with cells transiently treated with hydrogen peroxide (H<sub>2</sub>O<sub>2</sub>). In H<sub>2</sub>O<sub>2</sub>-treated cells, we observed a more dramatic increase in calcium, much higher than what was seen in the case of cells shifted to glutathione-free medium (Figure 2A). To examine whether this difference in calcium influx that was being observed in H<sub>2</sub>O<sub>2</sub>-treated and glutathione-depleted cells might be due to the differences in the redox environments being created in the two situations, we measured the cytoplasmic redox state using the redox probe, Grx1-roGFP2. This probe is a fusion protein containing roGFP2 genetically fused to redox enzyme glutaredoxin-1 for measurement of glutathione redox potential (Gutscher *et al.*, 2008). We observed that, while H<sub>2</sub>O<sub>2</sub> created an almost immediate and significant increase in the oxidized state of the cytoplasm, *gsh1Δ* cells showed a slow increase in the oxidized state upon transfer of the cells to a glutathione-free medium (Figure 2B). This seemed to indicate a correlation between the redox state of the cells and the calcium influx. To further confirm whether cytoplasmic calcium levels correlated with changes in the cellular redox state, we made use of the glutathione-degrading enzyme, ChaC1, that was recently described (Kumar *et al.*, 2012). This enzyme specifically acts on reduced glutathione, not on oxidized glutathione (Tsunoda *et al.*, 2014; Kaur *et al.*, personal communication), and expression of ChaC1 in yeast cells therefore leads to a selective depletion of reduced glutathione

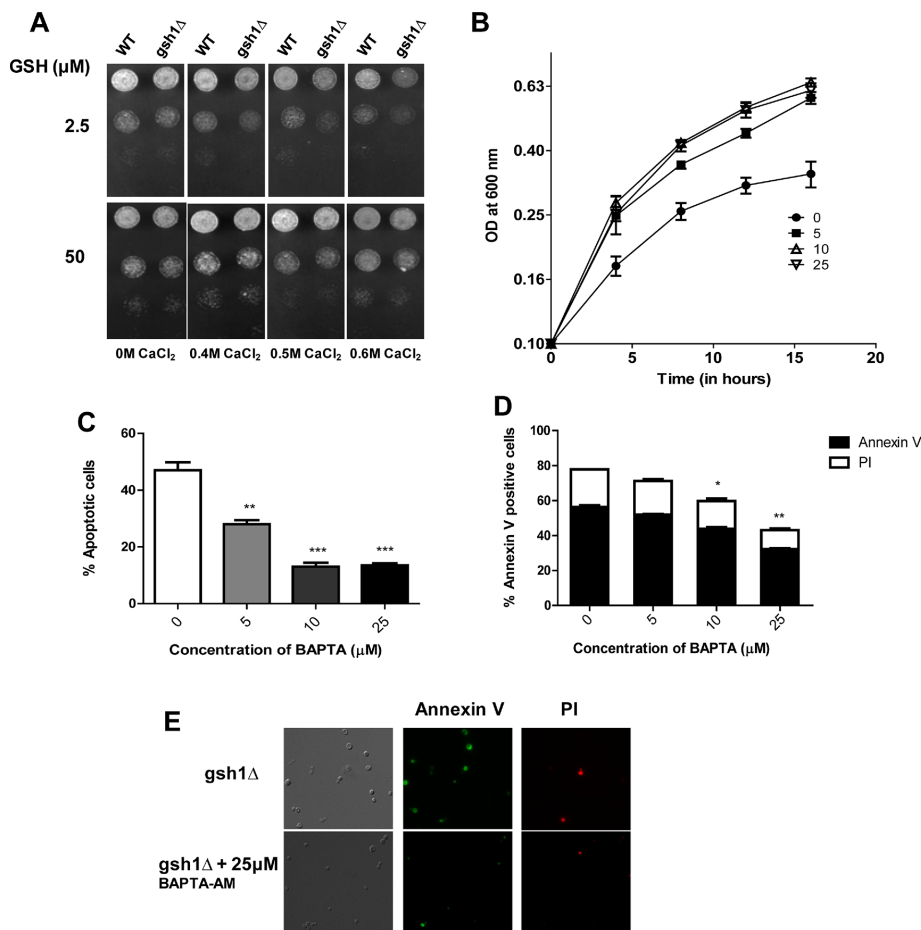


**FIGURE 1:** Glutathione-depleted cells are more sensitive to calcium stress. (A) The *S. cerevisiae* WT and *gsh1Δ* strains were grown to exponential phase in minimal medium containing 100  $\mu\text{M}$  glutathione, harvested, washed, resuspended in water, and serially diluted to give 0.1, 0.01, 0.001, and 0.0001 A600 of cells. Ten microliters of these dilutions was spotted on minimal medium containing 0.4, 0.5, and 0.6 M  $\text{CaCl}_2$  each at 5 and 50  $\mu\text{M}$  glutathione. The photographs were taken after 2 d of incubation at 30°C. (B) *gsh1Δ* strain was grown in the absence of glutathione and in the presence of different concentrations of BAPTA-AM (0, 5, 10, and 25  $\mu\text{M}$ ). Growth curve was plotted by taking OD<sub>600nm</sub> at 4 h intervals for 16 h until the cells reached stationary phase. The bars correspond to the mean of three independent experiments  $\pm$  SD. (C) Cellular DNA fragmentation assay. *gsh1Δ* cells grown in the absence of glutathione and in the presence of different concentrations of BAPTA-AM were harvested at 12 h, and equal OD of cells were taken and stained for DNA fragmentation with TUNEL reaction containing fluorescently tagged dUTP. Quantification of apoptotic cells; % positive cells was determined from >100 cells from different field views. Error bars correspond to the mean of three independent experiments  $\pm$  SD. Statistical difference: \*\* $p < 0.01$ ; \*\*\* $p < 0.001$ . (D) Annexin V staining for exposition of phosphatidylserine at membrane surface. *gsh1Δ* cells grown in the absence of glutathione and in the presence of different concentrations of BAPTA-AM were harvested at 12 h, and equal OD of cells were taken and stained with Alexa Fluor 488-labeled Annexin V and PI. Quantitation of apoptotic cells; % of Annexin V-positive cells and dead cells; % of PI positive was done by flow-cytometric analysis. Results are represented as a histogram. The results reported are from three independent experiments. (E) Fluorescence and differential interface-contrast micrographs showing apoptotic cells as Annexin (+) PI (-) and dead cells as Annexin (+) PI (+).

that leads to a higher oxidizing environment. We measured the redox in ChaC1-overexpressing cells and observed that ChaC1 overexpression led to a significantly higher oxidizing environment, as seen from the redox measurements (Figure 2B). Interestingly, the ChaC1-overexpressing cells also displayed a higher intracellular calcium influx compared with what was seen in the *gsh1Δ* background with vector alone. We also compared this overexpression of ChaC1

in a wild-type (WT) background, examining both the redox state of the cytoplasm and the cytoplasmic calcium influx (Figure 2A). The results clearly indicate a close correlation between the redox state and calcium influx in the cell.

**The vacuolar Yvc1p and the plasma membrane Cch1p are the major calcium channels responding to the redox environment leading to cytoplasmic calcium influx**

*S. cerevisiae* has several calcium channels and transporters located in different organelles. (Cui *et al.*, 2009a,b) Two of these channels are mainly responsible for calcium influx into the cytoplasm: Yvc1p, which is a vacuolar channel, and Cch1p, which is on the plasma membrane. To determine which of the transporter channels was playing a key role in the influx of calcium during glutathione depletion, we created *gsh1Δ* deletions in the transporter deletion backgrounds. In these backgrounds, we also overexpressed mammalian ChaC1 to obtain clearer phenotypes on glutathione-limited plates. We observed that disruption of either the *YVC1* or *CCH1* genes led to a significant rescue in the growth on the glutathione-depletion medium. Further, the double deletion *cch1Δ yvc1Δ* showed an enhanced growth and rescue (Figure 3A). This suggested that both Yvc1p and Cch1p were contributing to the flux of calcium in the cell upon glutathione depletion.

The growth phenotypes seen on the plates were further confirmed by actual measurement of intracellular calcium levels. Using the aequorin assay, we were able to observe lesser influx of intracellular calcium in both the *cch1Δ* and *yvc1Δ* strains, and this effect was more accentuated in the *cch1Δ yvc1Δ* double-deletion background (Figure 3B). These results confirm the involvement of both these transporters in increasing  $\text{Ca}^{2+}$  levels in the cell upon glutathione depletion.

**Calcium sensitivity of the glutathione-depleted cells is independent of the calcium transcriptional regulator, CRZ1**

Unlike the rapid and immediate rise in calcium levels under oxidative stress induced by  $\text{H}_2\text{O}_2$ , the increase in calcium levels seen with the *S. cerevisiae gsh1Δ* cells and in the

*S. cerevisiae gsh1Δ* cells with ChaC1 overexpression seemed more gradual. We therefore sought to examine whether this might be a consequence of transcriptional regulation. Transcriptional regulation of some calcium transporters (PMC1 and PMR1) is known to be mediated by the CRZ1 transcription factor (Yoshimoto *et al.*, 2002). If CRZ1 is involved in the response to glutathione depletion, then *S. cerevisiae* cells bearing the *crz1Δ* would also show some rescue

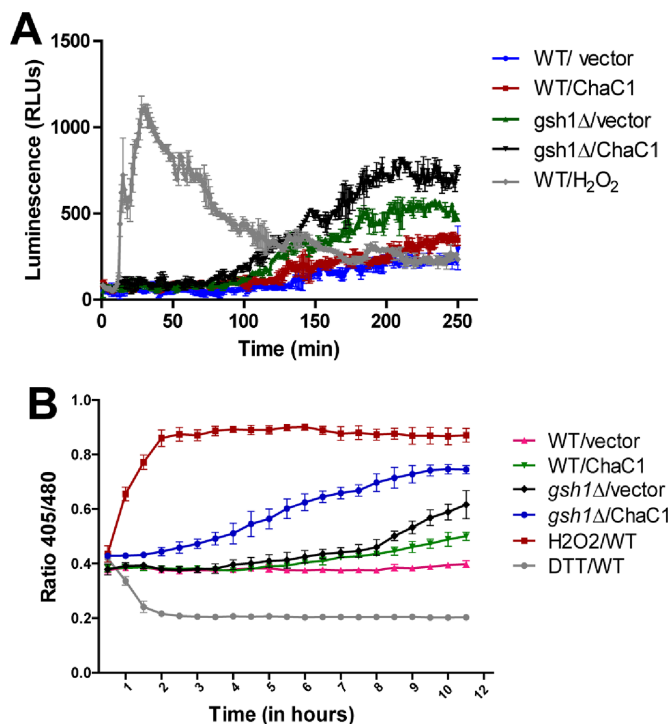


**FIGURE 2:** Glutathione (GSH) depletion by ChaC1 results in a more oxidizing environment: correlation with calcium flux. (A) Effect of ChaC1 overexpression on relative cytosolic Ca<sup>2+</sup> levels represented as luminescence units/s. WT and *gsh1Δ* cells expressing coelentrazine-reconstituted cytAEQ and transformed with vector and ChaC1 were grown in the absence of glutathione. Real-time calcium changes in the cytoplasm were monitored for 250 min. Each determination was repeated three times as a different experiment. RLU/s<sub>max</sub> values for each strain (obtained upon final detergent permeabilization and 10 mM CaCl<sub>2</sub> treatment) were 12,673 (WT/vector), 9934 (WT/ChaC1), 11,243 (*gsh1Δ*/vector), and 8995 (*gsh1Δ*/ChaC1). (B) Measurement of glutathione redox state using Grx1-roGFP<sub>2</sub>. WT and *gsh1Δ* cells transformed with vector and ChaC1 were grown in the absence of glutathione, and Grx1-roGFP<sub>2</sub> response was followed for 12 h. Exposure to 1.5 mM H<sub>2</sub>O<sub>2</sub> and 5 mM dithiothreitol was taken as a control for fully oxidized and fully reduced glutathione. The ratio of the fluorescence emission at 405–480 nm at fixed excitation of 510 nm is plotted against time. The graph shows the mean ratio of the readings from three independent experiments. Error bars represent SDs from the mean.

similar to *cch1Δ* or *yvc1Δ*. However, in the plate-based growth assays, no significant rescue could be observed in *crz1Δ* strain (Supplemental Figure 1a).

Because *YVC1* and *CCH1* appeared not to be regulated by *CRZ1*, we specifically evaluated whether *CCH1* and *YVC1* were regulated under oxidative stress using real-time quantitative PCR. However, no significant change in *CCH1* and *YVC1* mRNA levels was observed relative to unstressed cells. In contrast, *GSH1*, which is known to be up-regulated in oxidative stress, was used as a control and showed the expected increase in expression (Supplemental Figure 1b). These results seem to suggest that the effects of calcium influx that involve Yvc1p and Cch1p are not mediated by transcriptional regulation to any significant extent.

### Glutathione depletion leads to glutathionylation of Yvc1p

In the absence of any significant role of transcription in the process, we examined possible posttranslational modifications. Previ-

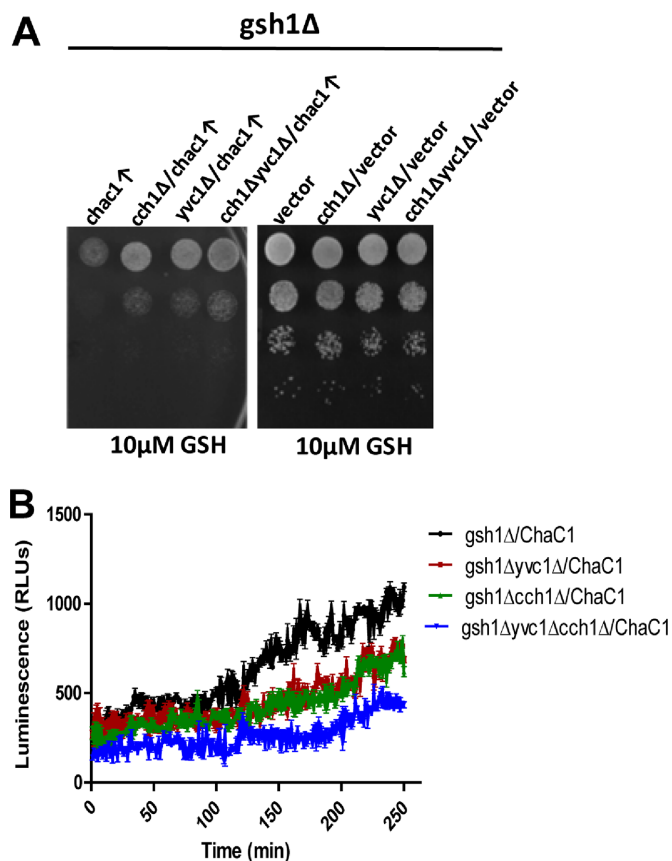


**FIGURE 3:** Calcium channel mutants rescue the effect of glutathione depletion. (A) Effect of ChaC1 overexpression-induced glutathione depletion on cell growth. Isogenic strains *gsh1Δ*, *gsh1Δcch1Δ*, *gsh1Δyvc1Δ*, and *gsh1Δcch1Δyvc1Δ* transformed with ChaC1 and vector control were spotted (10 μl) in 10-fold serial dilutions 0.1, 0.01, 0.001, and 0.0001 A<sub>600</sub> onto SD-Ura plates supplemented with 10 μM glutathione. The photographs were taken after 2 d of incubation at 30°C. (B) Relative cytosolic calcium levels represented as luminescence units/s in *gsh1Δ*, *gsh1Δcch1Δ*, *gsh1Δyvc1Δ*, and *gsh1Δyvc1Δcch1Δ* transformed with ChaC1. Each determination was repeated three times as an independent experiment. RLU/s<sub>max</sub> values for each strain (obtained upon final detergent permeabilization and 10 mM CaCl<sub>2</sub> treatment) were 11,643 (*gsh1Δ*), 9921 (*gsh1Δcch1Δ*), 11,213 (*gsh1Δyvc1Δ*), and 8225 (and *gsh1Δyvc1Δcch1Δ*). Error bars represent SDs from the mean.

ous studies have indicated that many of these transporters can be regulated by modification of the cysteine residues. In the present case, the redox state appeared to have an important role in regulating calcium levels, so we examined whether this regulation might be due to glutathionylation, since this posttranslational modification depends on the reduced glutathione:oxidized glutathione (GSH:GSSG) ratio in the cell. In this study, we decided to focus on the vacuolar calcium pump Yvc1p.

We first carried out *in vitro* experiments to determine whether Yvc1p can be glutathionylated. Yvc1p was His-tagged at the C-terminal, and the His-tagged Yvc1p functioned very similarly to untagged Yvc1p (unpublished data). His-tagged Yvc1p was used in all future experiments. The tagged Yvc1p expressed downstream of the constitutive TEF promoter was purified from yeast cell lysates (see *Materials and Methods*). The purified protein was treated with 1 mM GSH and 400 μM diamide. Glutathionylated Yvc1p was detected using Western blot

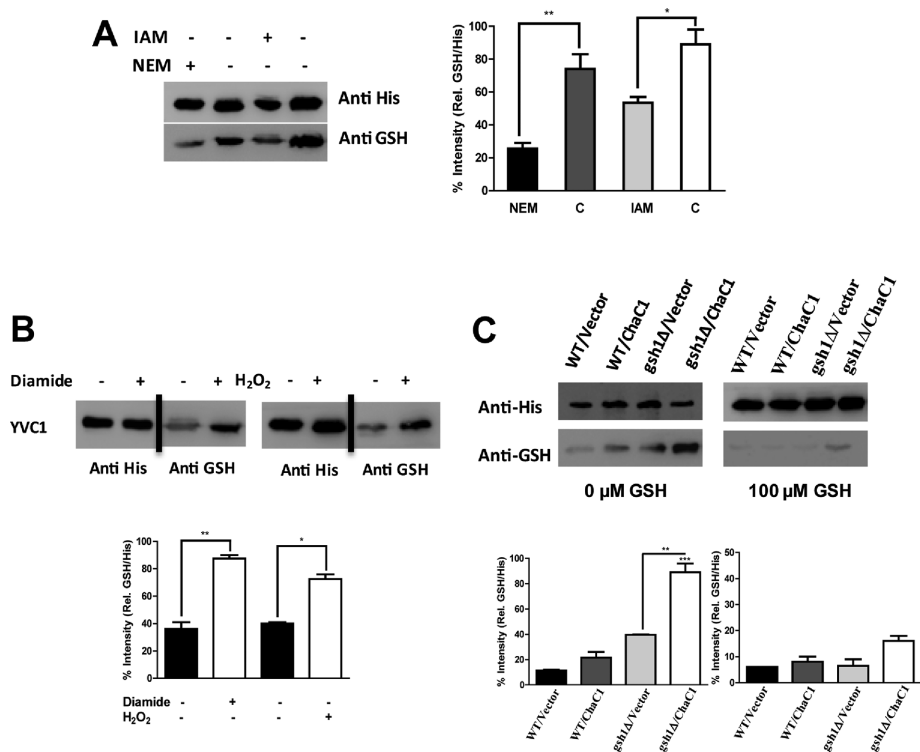


**FIGURE 4:** Yvc1p glutathionylation takes place under glutathione depletion. (A) In vitro glutathionylation analysis of Yvc1p. Purified Yvc1p was incubated with GSH (1 mM) and diamide (400 μM) in the presence and absence of cysteine modifying agents NEM and IAM and analyzed by Western blot. (B) Diamide and H<sub>2</sub>O<sub>2</sub> increase glutathionylation of Yvc1p in vivo. Cells overexpressing Yvc1p with OD = 1.5 were treated with diamide (1 mM) and H<sub>2</sub>O<sub>2</sub> (1.5 mM) for 20 min. After being washed, cells were lysed using glass beads, and His-tagged Yvc1p protein was purified using Ni-NTA beads and analyzed by Western blot. (C) Glutathione depletion influences the glutathionylation state of Yvc1p. WT and *gsh1Δ* strains overexpressing Yvc1p and transformed with ChaC1 and vector were cultured without and with 100 μM glutathione in medium. Cells were harvested at OD = 1.5. After being washed, cells were lysed using glass beads, and His-tagged Yvc1p protein was purified using Ni-NTA beads and analyzed by Western blot. Western analysis of the above experiments was carried with an equal amount of protein resolved using 10% SDS-PAGE and electroblotted on nitrocellulose membrane. The blots were probed with mouse anti-His and mouse anti-GSH primary antibodies and goat anti-mouse HRP-conjugated IgG as secondary antibody. The signal was detected using Luminata forte Western HRP substrate. The total protein expression was then quantified by densitometry analysis of protein bands. The data are expressed as the percentage protein expression compared with control (Anti HIS) expression level and are the mean ± SD of three independent experiments. Statistical difference: \*,  $p < 0.05$ ; \*\*,  $p < 0.01$ ; \*\*\*,  $p < 0.001$ .

analysis with anti-GSH antibody, and significant glutathionylation was observed. Blocking cysteine residues by pretreatment with alkylating agents like *N*-ethylmaleimide (NEM) and iodoacetamide (IAM) significantly reduced Yvc1p glutathionylation (Figure 4A).

To examine possible glutathionylation in vivo, we exposed Yvc1p-overexpressing yeast cells to two oxidizing agents, diamide and H<sub>2</sub>O<sub>2</sub>. In both cases, a significant increase in the levels of Yvc1p glutathionylation was observed (Figure 4B). To examine whether this was also observed under conditions of intracellular glutathione depletion, we analyzed Yvc1p glutathionylation in ChaC1-overexpressing *gsh1Δ* cells using anti-GSH and anti-His antibody. Notably, a significant increase in the levels of Yvc1p glutathionylation was observed in ChaC1-overexpressing cells as compared with vector control, suggesting that Yvc1p was glutathionylated in vivo upon glutathione depletion (Figure 4C).

### Yvc1p is regulated by specific glutathionylation at the residues Cys-17, Cys-79, and Cys-191

Yvc1p has nine cysteine residues, eight of which are cytoplasmic and thus accessible to glutathionylation. Only Cys-343 is not cytoplasmic and is localized within TMD2 (Figure 5A). Sequence comparisons among fungi revealed that, among these cytoplasmic cysteines, only Cys-191 was conserved among the yeast and fungi.

To identify which of these cysteines might be involved in the glutathionylation of Yvc1p, we individually mutated each of the nine cysteines to alanine. To evaluate the activity of each mutant, we used H<sub>2</sub>O<sub>2</sub> sensitivity as an assay for functionality. WT Yvc1p shows sensitivity to oxidative stress, while the *yvc1Δ* shows resistance. Using these as reference points, all the individual Yvc1p mutants expressed from the TEF promoter were transformed into the *yvc1Δ* background strain and checked for sensitivity to H<sub>2</sub>O<sub>2</sub>. We observed that five of the mutants, C17A, C61A, C79A, C179A, and C191A showed a loss of activity and phenotypically behaved like loss-of-function mutants (Figure 5B). In contrast, C343A showed a gain of function, appearing hypersensitive (Figure 5). Control spotting of untreated cells showed no growth difference (Supplemental Figure 2a).

For determination of whether the altered activity of these mutants might be due to their mislocalization, immunostaining was performed (Supplemental Figure 3). The mutants C17A, C79A, C104A, C132A, C191A, and C624A appeared to be correctly localized to the vacuole. However, C61A and C179A did not appear to be correctly localized to the vacuole, which explained the loss of function (Supplemental Figure 3). C343A, in contrast, was localized partially to the plasma membrane. This would allow it to access the higher extracellular pools, which might explain the hypersensitivity of C343A. All these mutants, C61A, C179A, and C343A, were not pursued further.

To obtain better insights into the functional activity of these mutants, we used aequorin-based calcium assays for the remaining three loss-of-function mutants C17A, C79A, and C191A. In the aequorin-based calcium assay, all the three cysteine mutants showed less activity than the control Yvc1p. The defect appeared more severe in C17A and C191A and less severe in C79A (Figure 5C).

To determine whether the loss of function correlated with the loss in glutathionylation, we also assessed levels of glutathionylation in the mutant proteins purified from yeast cells exposed to oxidative stress (H<sub>2</sub>O<sub>2</sub>). The mutants C104A, C132A, C343A, and C624A were found to have similar glutathionylation levels as WT, whereas the mutants C17A, C79A, and C191A had significantly lower levels (Figure 5D). In addition to suggesting the involvement of these three residues in glutathionylation, this also indicated that no single cysteine was involved and that more than one cysteine is the target

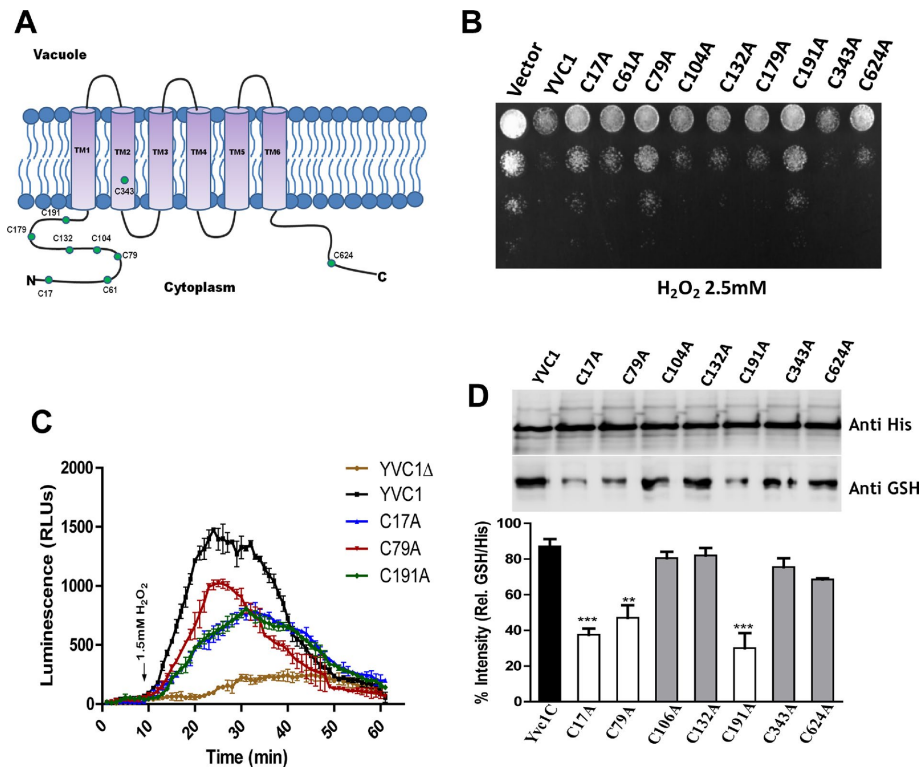


**FIGURE 5:** Site specific glutathionylation takes place in Yvc1p. (A) Functional characterization of cysteine to alanine mutants. Empty vector (pRS313TF), WT (YVC1), and all the nine cysteine to alanine mutants were transformed in a *yvc1Δ* strain. Transformants were grown to exponential phase in minimal medium, exposed to 2.5 mM H<sub>2</sub>O<sub>2</sub>, washed, serially diluted, and spotted on minimal media plates. The photographs were taken after 2–3 d of incubation at 30°C. (B) Topological model predicting the location of nine cysteines present in YVC1. (C) Functional assay of WT and defective mutants under exogenous oxidative stress. Aequorin-based intracellular calcium measurement done using aequorin coding pEVP11/AEQ plasmid cotransformed with empty vector (pRS313TF), WT (YVC1), and all the nine cysteine to alanine mutants (data shown only for three) in a *yvc1Δ* strain. Exogenous stress of 1.5 mM H<sub>2</sub>O<sub>2</sub> was given after 10 min, and relative calcium levels were monitored up to 60 min. Each determination was repeated three times as an independent experiment. RLU/s<sub>max</sub> values for each strain (obtained upon final detergent permeabilization and 10 mM CaCl<sub>2</sub> treatment) were 14,228 (*yvc1Δ*), 14,547 (YVC1), 13,162 (C17A), 14,829 (C79A), and 13,732 (C191A). Error bars represent SDs from the mean. (D) Glutathionylation analysis of Yvc1p mutants. YVC1 and mutant proteins were purified from a *yvc1Δ* strain overexpressing WT (YVC1) and all the nine cysteine to alanine mutants after exposure to 1.5 mM H<sub>2</sub>O<sub>2</sub> for 20 min. Cells were harvested at OD = 1.5. After being washed, cells were lysed using glass beads, and His-tagged protein was purified using Ni-NTA beads and analyzed by Western blot. Western analysis in the above experiments was carried with equal amount of protein resolved using 10% SDS–PAGE and electroblotted on nitrocellulose membrane. The blots were probed with mouse anti-His and mouse anti-GSH primary antibodies and goat anti-mouse HRP-conjugated IgG as secondary antibody. The signal was detected using Luminata forte Western HRP substrate. The total protein expression was then quantified by densitometry analysis of protein bands. The data are expressed as the percentage protein expression compared with control (Anti HIS) expression level and are the mean ± SD of two independent experiments. Statistical difference: \*\*,  $p < 0.05$ ; \*\*\*,  $p < 0.001$ .

of glutathionylation. For confirmation, double mutants C17A C79A, C17A C191A, and C79A C191A and a triple mutant C17A C79A C191A were generated and analyzed for functionality and glutathionylation. In the H<sub>2</sub>O<sub>2</sub> sensitivity assay, the double mutants showed better growth than the single mutants, and the triple mutant behaved almost like the *yvc1Δ* strain in terms of growth (Figure 6A). Control spotting of untreated cells showed no growth difference (Supplemental Figure 2b). These were then analyzed more rigorously for function by their ability to transport calcium using the aequorin assay. The intracellular influx of calcium decreased in the

double mutants C17A C79A, C17A C191A, and C79A C191A and was still low in the triple mutant C17A C79A C191A, which is comparable to *yvc1Δ* (Figure 6B). No defect in vacuolar localization was observed in the triple cysteine mutant C17A C79A C191A (Figure 6C). To examine these mutants for their glutathionylation patterns, we carried out a glutathionylation analysis. The profiles revealed significantly lower levels of glutathionylation in the double mutants and almost no glutathionylation in the triple mutant. These results, correlated with the functional analysis, suggested the glutathionylation of these specific cysteines in Yvc1p regulation (Figure 6D) and is shown schematically in Figure 6E.

### Regulation of Yvc1p by hyperosmolarity is also dependent on activation of Yvc1p by glutathionylation

Yvc1p is known to be a mechanosensitive calcium channel. Mechanosensitivity can be evaluated by osmotic force (Denis and Cyert, 2002; Zhou et al., 2003). To determine whether the activation of Yvc1p by hyperosmotic pressure was also occurring through glutathionylation, we examined the glutathionylation status of Yvc1p under osmotic stress, that is, 0.8 M NaCl, and observed a significant increase in the glutathionylation of Yvc1p (Figure 7A). To correlate it with the redox state in the cell, we also measured the cytoplasmic redox state using the redox probe cytoGrx1-roGFP under osmotic stress. Rapid change in the redox state was observed when cells were exposed to 0.8 M NaCl (Figure 7B). Further, we checked the activity of the WT transporter and triple cysteine mutant under osmotic stress using the aequorin calcium assay. Significantly decreased calcium signal was observed (Figure 7C), which indicates that the mechanosensitivity of Yvc1p is also being largely mediated through a redox-dependent mechanism.

### The yeast glutathione S-transferase Gtt1p is required for glutathionylation and activation of Yvc1p

Glutathionylation of proteins has been shown to occur either enzymatically or non-enzymatically (Mailloux et al., 2014). In mammalian cells, the proteins known to catalyze glutathionylation have been shown to be either the glutathione S-transferases (belonging to the omega and pi family; Manevich et al., 2004; Menon and Board, 2013) or the glutaredoxins (Starke et al., 2003).

When we examined the genome of *S. cerevisiae*, we found it has three reported glutathione transferases related to the GST omega family. These are GTO1, which is peroxisomal, and GTO2 and GTO3 (Barreto et al., 2006). Two other proteins with a GST domain that has no similarity to mammalian GSTs but is related to the bacterial GSTs

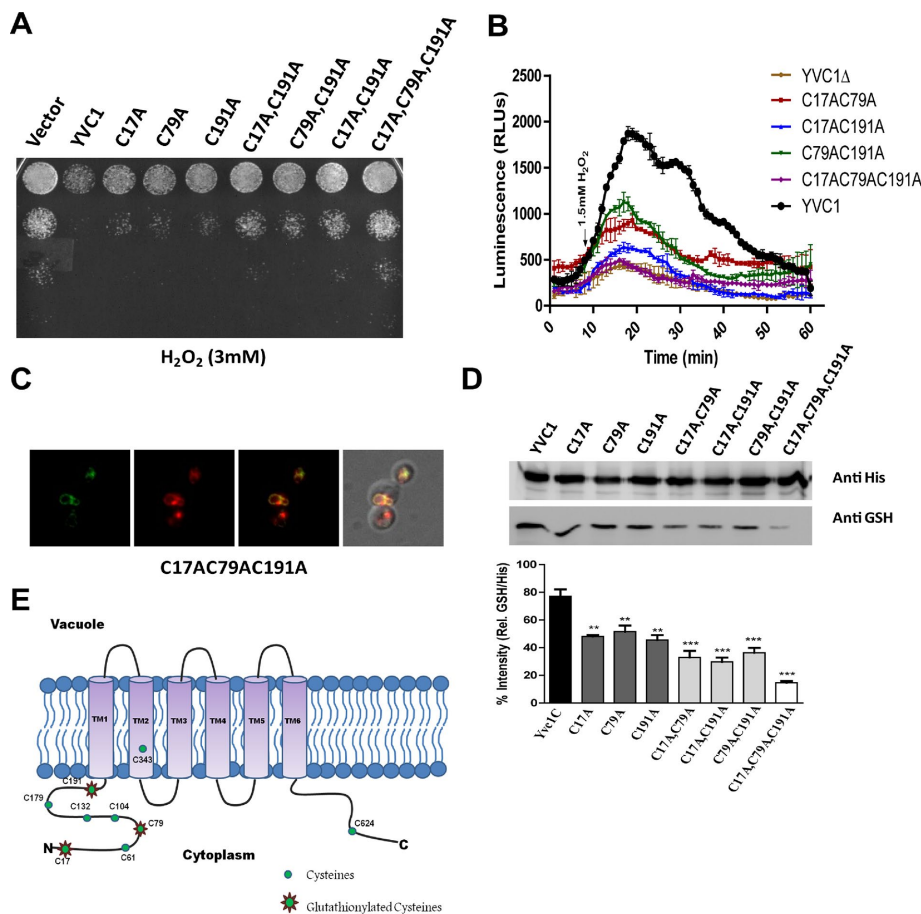


**FIGURE 6:** Specific cysteine residues are glutathionylated in Yvc1p. (A) Functional characterization of cysteine to alanine double and triple mutants. Empty vector (pRS313TF), WT (YVC1), and a combination of double mutants C17AC79A, C17AC191A, C79AC191A, and triple mutant C17AC79AC191A were transformed in a *yvc1Δ* strain. Transformants were grown to exponential phase in minimal medium, exposed to 3 mM H<sub>2</sub>O<sub>2</sub>, washed, serially diluted, and spotted on minimal media plates. The photographs were taken after 2–3 d of incubation at 30°C. (B) Functional assay of WT, double mutants, and triple mutant under exogenous oxidative stress. Aequorin-based intracellular calcium measurement done using aequorin coding pEVP11/AEQ plasmid cotransformed with Empty vector (pRS313TF), WT (YVC1), and all double mutants and a triple mutant in *yvc1Δ* strain. Exogenous stress of 1.5 mM H<sub>2</sub>O<sub>2</sub> was given after 10 min, and relative calcium levels were monitored up to 60 min. Each determination was repeated three times as an independent experiment. RLU/s<sub>max</sub> values for each strain (obtained upon final detergent permeabilization and 10 mM CaCl<sub>2</sub> treatment) were 15,438 (*yvc1Δ*), 15,923 (YVC1), 13,423 (C17AC79A), 14,274 (C17AC191A), 13,983 (C79AC191A), and 14,289 (C17AC79AC191A). Error bars represent SDs from the mean. (C) Vacuolar localization of C17AC79AC191A mutant. (D) Glutathionylation analysis of Yvc1p mutants. YVC1 and mutant protein was purified from a *yvc1Δ* strain overexpressing WT (YVC1), single mutants C17A, C79A, C191A, double mutants C17AC79A, C17AC191A, C79AC191A, and triple mutant C17AC79AC191A after exposure to 1.5 mM H<sub>2</sub>O<sub>2</sub> for 20 min. Cells were harvested at OD = 1.5. After being washed, cells were lysed using glass beads and His-tagged protein was purified using Ni-NTA beads and analyzed by Western blot. Western analysis in the above experiments was carried with an equal amount of protein resolved using 10% SDS-PAGE and electroblotted on nitrocellulose membrane. The blots were probed with mouse anti-His and mouse anti-GSH primary antibodies and goat anti-mouse HRP-conjugated IgG as secondary antibody. The signal was detected using Luminata forte Western HRP substrate. The total protein expression was then quantified by densitometry analysis of protein bands. The data are expressed as the percentage protein expression compared with control (Anti HIS) expression level and are the mean ± SD of two independent experiments. Statistical difference: \*\*, *p* < 0.01; \*\*\*, *p* < 0.001. (E) Model predicting the location of cysteines involved in glutathionylation and activation of YVC1.

are the glutathione transferases GST1 and GST2 (Choi *et al.*, 1998). Finally, the two glutaredoxins, GRX1 and GRX2, have also been reported to have glutathione S-transferase activity (Collinson and

might be involved in the process. The thioredoxins, glutaredoxins, and sulfiredoxins are possible candidate enzymes involved in de-glutathionylation (Jung and Thomas, 1996; Findlay *et al.*, 2006). We

Grant, 2003). In the absence of any prior information on the role of these proteins in glutathionylation in yeast, we evaluated each of these for their role in glutathionylation. GST1 and GST2 have been shown to function as glutathione transferases through enzymatic glutathione-conjugation activity against a known substrate, ethacrynic acid (but not the classical substrate CDNB; Choi *et al.*, 1998). To examine whether these transferases had a role in the activation of Yvc1p, we examined glutathionylation in the deletion backgrounds of all the potential glutathione transferases *gtt1Δ*, *gtt2Δ*, *gto1Δ*, *gto2Δ*, *gto3Δ*, *grx1Δ*, and *grx2Δ*. We observed that glutathionylation of Yvc1p is dramatically reduced in the *gtt1Δ* background (Figure 8A). In contrast *gto1Δ*, *gto2Δ*, *gto3Δ*, *gtt2Δ*, *grx1Δ*, and *grx2Δ* had no significant effect on the glutathionylation of Yvc1p (Supplemental Figure 4). To see whether the absence of glutathionylation seen in the *gtt1Δ* mutant was reflected in the calcium release, we analyzed the release of intracellular calcium by Yvc1p upon oxidative stress in the *gtt1Δ* background. We observed that, in *gtt1Δ*, very low calcium influx was seen relative to the WT, further confirming that the activation of Yvc1p was occurring by glutathionylation mediated by Gtt1p (Figure 8B).

### Yvc1p glutathionylation is reversible: de-glutathionylation is primarily mediated by the thioredoxin Trx2p

During the activation of Yvc1p under oxidative stress, we observed the restoration of calcium levels with time. This could be a result of removal of the excess calcium by pumps effluxing Ca<sup>2+</sup> out of the cytoplasm. It could also be a consequence of the deactivation of the Yvc1p by possible de-glutathionylation. To get a better understanding of this, we investigated the glutathionylation status of Yvc1p at different time intervals under oxidative stress generated by H<sub>2</sub>O<sub>2</sub>. Cells were exposed to H<sub>2</sub>O<sub>2</sub> for different time periods, spun down, washed, and analyzed. We observed that, after an initial increase, the glutathionylation levels of Yvc1p came down significantly at more prolonged time periods (Figure 8C). The protein levels, however, remain relatively unchanged. These results indicate that glutathionylated Yvc1p is deactivated by de-glutathionylation so that Yvc1p eventually is restored to its resting state.

To examine whether this Yvc1p de-glutathionylation is enzyme dependent, we examined the possible candidate proteins that

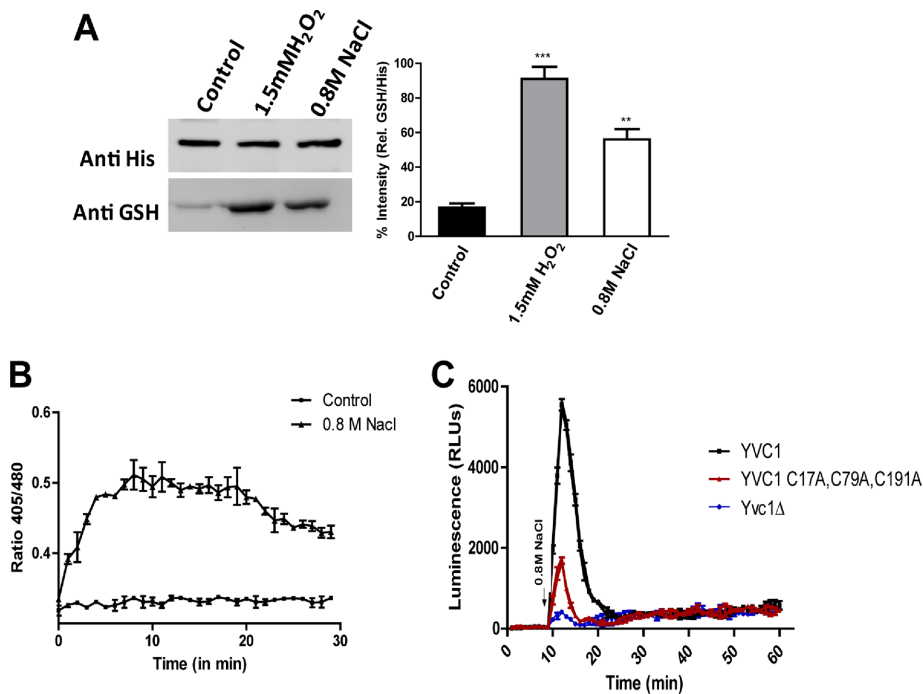


**FIGURE 7:** Osmotic stress induces redox-dependent glutathionylation of YVC1. (A) Osmotic stress induces glutathionylation of Yvc1p. Yvc1Δ cells overexpressing Yvc1p at OD = 1.5 were exposed to 0.8 M NaCl for 5 min. After being washed, cells were lysed using glass beads, and His-tagged Yvc1p protein was purified using Ni-NTA beads and analyzed by Western blot. A 1.5 mM H<sub>2</sub>O<sub>2</sub> exposure was taken as positive control for glutathionylation. Western analysis in the above experiments was carried with equal amount of protein resolved using 10% SDS-PAGE and electroblotted on nitrocellulose membrane. The blots were probed with mouse anti-His and mouse anti-GSH primary antibodies and goat anti-mouse HRP-conjugated IgG as secondary antibody. The signal was detected using Luminata forte Western HRP substrate. The total protein expression was then quantified by densitometry analysis of protein bands. The data are expressed as the percentage protein expression compared with control (Anti HIS) expression level and are the mean ± SD of three independent experiments. Statistical difference: \*\*,  $p < 0.01$ ; \*\*\*,  $p < 0.001$ . (B) Osmotic stress changes the redox state of glutathione in the cell. Measurement of glutathione redox state using Grx1-roGFP2. WT cells (BY4741) grown in YPD were exposed to 0.8 M NaCl, and Grx1-roGFP2 response was followed for 30 min. Ratio of the fluorescence emission at 405–480 nm at fixed excitation of 510 nm is plotted against time. The graph shows the mean ratio of the readings from three independent experiments. (C) Functional assay of WT and triple cysteine mutant under osmotic stress. Aequorin-based intracellular calcium measurement done using aequorin coding pEVP11/AEQ plasmid cotransformed with Empty vector Yvc1Δ (pRS313TF), WT (YVC1), and triple cysteine mutant in yvc1Δ strain. Osmotic stress of 0.8 M NaCl was given after 10 min, and relative calcium levels were monitored up to 60 min. Each determination was repeated three times as an independent experiment. RLU/s<sub>max</sub> values for each strain (obtained upon final detergent permeabilization and 10 mM CaCl<sub>2</sub> treatment) were 15,328 (yvc1Δ), 13,729 (YVC1), and 13,284 (C17AC79AC191A). Error bars represent SDs from the mean.

expressed the Yvc1p protein in the different glutaredoxin (*grx1Δ* and *grx2Δ*), thioredoxin (*trx1Δ* and *trx2Δ*), and sulfiredoxin (*srx1Δ*) mutant backgrounds and examined the glutathionylation status of Yvc1p. Among the different mutants, we observed that the *trx2Δ* mutant, and to a lesser extent the *trx1Δ* mutant, showed increased glutathionylation (Figure 8D). The sulfiredoxin deletion (*srx1Δ*) also showed increased glutathionylation as compared with WT but less than *trx2Δ* (Supplemental Figure 5). On the other hand, *grx1Δ* and *grx2Δ* had no significant effect on the glutathionylation of Yvc1p (Supplemental Figure 4). We evaluated these mutants for their ability to affect growth and calcium flux into the cell. *gsh1Δ* *trx2Δ* showed an enhanced growth defect on glutathione-limited plates (Supplemental Figure 6). Further, we observed that the *trx2Δ* mutant had high levels of Ca<sup>2+</sup> accumulation, and the signal was prolonged

(Figure 8E). This is expected if the protein Trx2p has a role in Yvc1p deglutathionylation, resulting in a prolonged activation and extended calcium efflux into the cytoplasm.

## DISCUSSION

In this paper, we have investigated in detail how glutathione depletion can lead to an increase in cytoplasmic calcium, a key event for the onset of apoptosis. Our results reveal how, during glutathione depletion, the yeast vacuolar calcium channel Yvc1p is activated by enzymatic glutathionylation at specific residues leading to the flux of calcium into the cytoplasm. The process is reversible, and the glutathione groups can be removed, again by enzymatic deglutathionylation, leading to deactivation and the restoration of the channel to its resting state (Figure 9).

YVC1 is a member of the TRP family of ion channels, which are known to be multimodal, in that they respond to a variety of environmental stimuli through different mechanisms. The mammalian TRP ion channel family is a large superfamily divided into six subfamilies: TRPA, TRPC, TRPV, TRPM, TRPP, and TRPML (Clapham, 2003). A few are known to be affected by the redox environment and thus are thought to function as redox sensors; however, the mechanisms of activation and response seems to be quite varied. The TRPM2 channels are activated by H<sub>2</sub>O<sub>2</sub> through binding to adenosine diphosphoribose (Clapham, 2003; Clapham *et al.*, 2005). TRPA1 and TRPV1 responds to diverse pungent chemicals, and their activation is mediated through covalent modification of cysteines (Bandell *et al.*, 2004; Jordt *et al.*, 2004; Macpherson *et al.*, 2005, 2007). Members of the TRPC and TRPV subfamilies, specifically TRPC5 and TRPV1 channels, are shown to be activated by nitrosylation and disulphide-bond formation (Yoshida *et al.*, 2006; Ogawa *et al.*, 2016). Very recently glutathionylation was also shown to be involved in TRPC5 activation (Hong *et al.*, 2015). The yeast *S. cerevisiae* has a single TRP channel, YVC1 (TRPY1), which can be functionally assayed by simple assays and could be a useful model for dissecting out TRP channel regulation.

The mechanism and the specificity of glutathionylation is still only poorly understood. Enzyme-independent glutathionylation is only favorable when the GSH:GSSG ratio falls to 100-fold lower than the reported levels in the cytoplasm (Gilbert, 1990). The enzymes largely thought to be responsible for the glutathionylation reaction are the glutathione S-transferases (GSTs). In mammalian cells, GST pi (GSTπ), and omega class GST (GSTO1-1), are thought to have an important role to play in glutathionylation under oxidative stress (Townsend *et al.*, 2009; Menon and Board, 2013). However, these did not appear to play a role in Yvc1p activation. In contrast, GST1, which is not known to have any thiol transferase activity, surprisingly

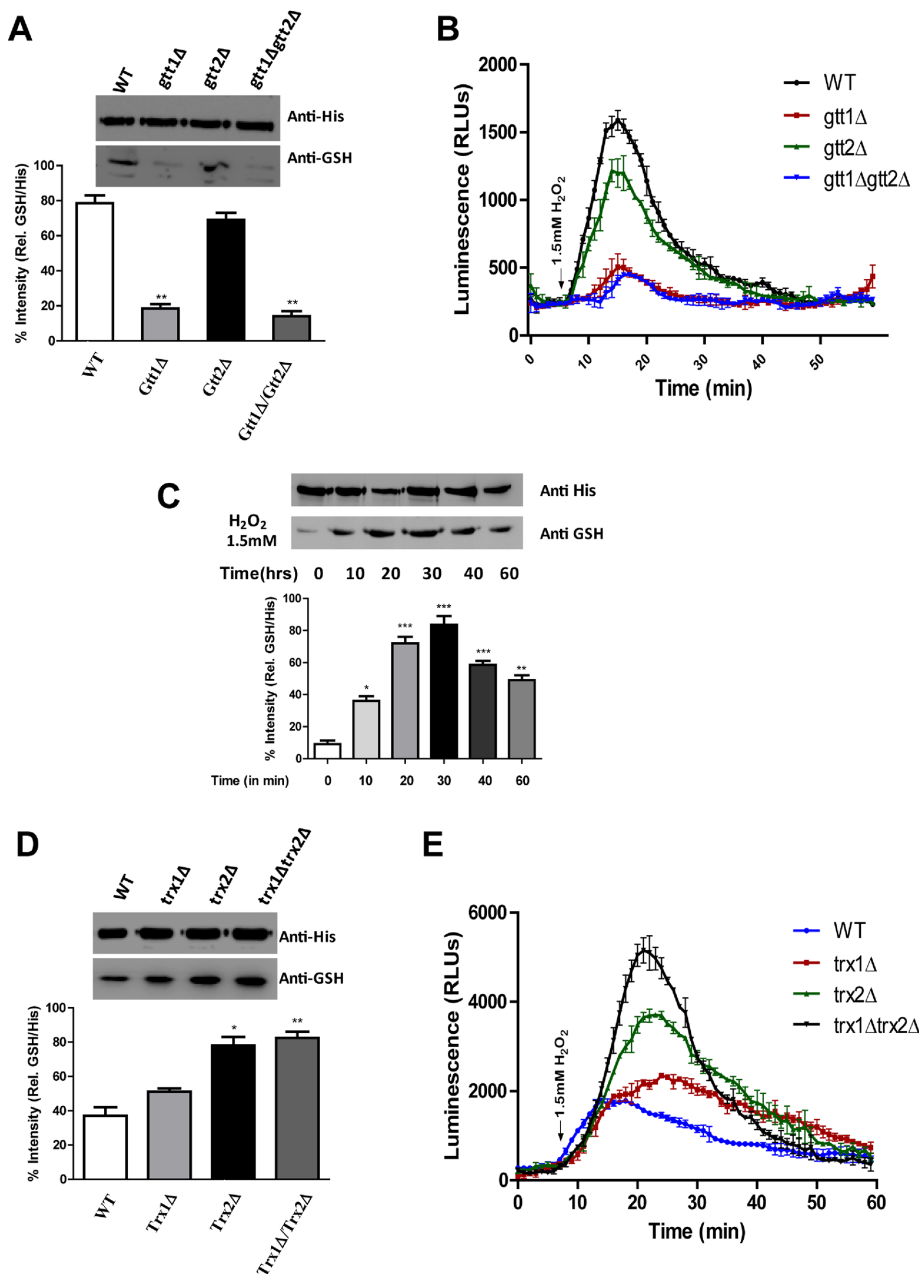


**FIGURE 8:** Yvc1p deglutathionylation is dependent on thioredoxins. (A, D) Glutathionylation analysis of Yvc1p in GST and TRX mutants. Yvc1p protein is purified from thioredoxin *trx1Δ*, *trx2Δ*, *trx1Δtrx2Δ* and glutathione S-transferase *gtt1Δ*, *gtt2Δ*, *gtt1Δgtt2Δ* mutants after exposure to 1.5 mM H<sub>2</sub>O<sub>2</sub> for 20 min. Cells were harvested at OD = 1.5. After being washed, cells were lysed using glass beads, and His-tagged protein was purified using Ni-NTA beads and analyzed by Western blot. Western analysis in the above experiments was carried out with an equal amount of protein resolved using 10% SDS-PAGE and electroblotted on nitrocellulose membrane. The blots were probed with mouse anti-His and mouse anti-GSH primary antibodies and goat anti-mouse HRP-conjugated IgG as secondary antibody. The signal was detected using Luminata forte Western HRP substrate. The total protein expression was then quantified by densitometry analysis of protein bands. The data are expressed as the percentage protein expression compared with control (Anti HIS) expression level and are the mean ± SD of three independent experiments. Statistical difference: \*\*,  $p < 0.01$ ; \*\*\*,  $p < 0.001$ . (B) Calcium measurement in *gtt1Δ*, *gtt2Δ*, and *gtt1Δgtt2Δ* relative to intracellular calcium levels were measured. Each determination was repeated three times as an independent experiment. (C) Time-dependent glutathionylation of Yvc1p. Glutathionylation analysis of Yvc1p in cells with OD = 1.5 and treated with H<sub>2</sub>O<sub>2</sub> (1.5 mM) for different time intervals from 0 to 60 min. After being washed, cells were lysed using glass beads, and His-tagged YVC1 protein was purified using Ni-NTA beads. Western analysis was done using anti-His and anti-glutathione antibody. (E) Calcium measurement in thioredoxin mutants. Isogenic strains WT (BY4741), *trx1Δ*, *trx2Δ*,

appeared to play a key role in the glutathionylation of Yvc1p. These findings should now enable one to dissect out the mechanisms by which glutathione S-transferases function in glutathionylation in vivo. Although some general rules have been suggested regarding the cysteines targeted for glutathionylation, predictions are still unreliable (Grek et al., 2013). In the present case, mutation in the three cysteines Cys-17, Cys-79, and Cys-191 showed loss of calcium channel activity and almost complete loss of glutathionylation of Yvc1p. Some residual glutathionylation was still observed, suggesting that perhaps some other residues might also contribute to some extent. Among these residues, only Cys-191 shows conservation among fungi. Although no cysteine is conserved among mammalian TRPs, all three cysteines are present in the N-terminal cytoplasmic region, similar to what has been observed with the N-terminal cysteines of mammalian TRPs (TRPA1, TRPV1, and TRPC5), which have also been shown to be redox sensitive (Salazar et al., 2008; Hong et al., 2015).

Deglutathionylation reactions have been more extensively investigated. Interestingly, although members of the thioredoxin superfamily (that includes thioredoxins, glutaredoxins, sulfiredoxins, GSTs, glutathione peroxidases, and protein disulfide isomerases) have been demonstrated to display deglutathionylation activity in vitro (Hayano et al., 1993; Jung and Thomas, 1996; Findlay et al., 2006), it is the glutaredoxins that are thought to be the key enzymes principally involved in deglutathionylation (Luikenhuis et al., 1998). Yeast has several glutaredoxins, of which GRX1 and GRX2 are cytoplasmic. We evaluated GRX1 and GRX2, the two cytosolic thioredoxins TRX1 and TRX2, and also yeast sulfiredoxin (SRX1), all of which have been shown to play a role in deglutathionylation in specific cases (Findlay et al., 2006). We made the very surprising observation that the yeast TRX2 protein is primarily involved in the deglutathionylation of the glutathionylated Yvc1p. It is interesting, in this context, that in a global

and *trx1Δtrx2Δ* were transformed with YVC1, and aequorin-based intracellular calcium measurement was done after exposure to 1.5 mM H<sub>2</sub>O<sub>2</sub> for 60 min. RLU/s<sub>max</sub> values for each strain (obtained upon final detergent permeabilization and 10 mM CaCl<sub>2</sub> treatment) were 12,322 (WT), 10,284 (*trx1Δ*), 8382 (*trx2Δ*), 9384 (*trx1Δtrx2Δ*), 11,372 (*gtt1Δ*), 12,843 (*gtt2Δ*), and 11,473 (*gtt1Δgtt2Δ*). Error bars represent SDs from the mean.

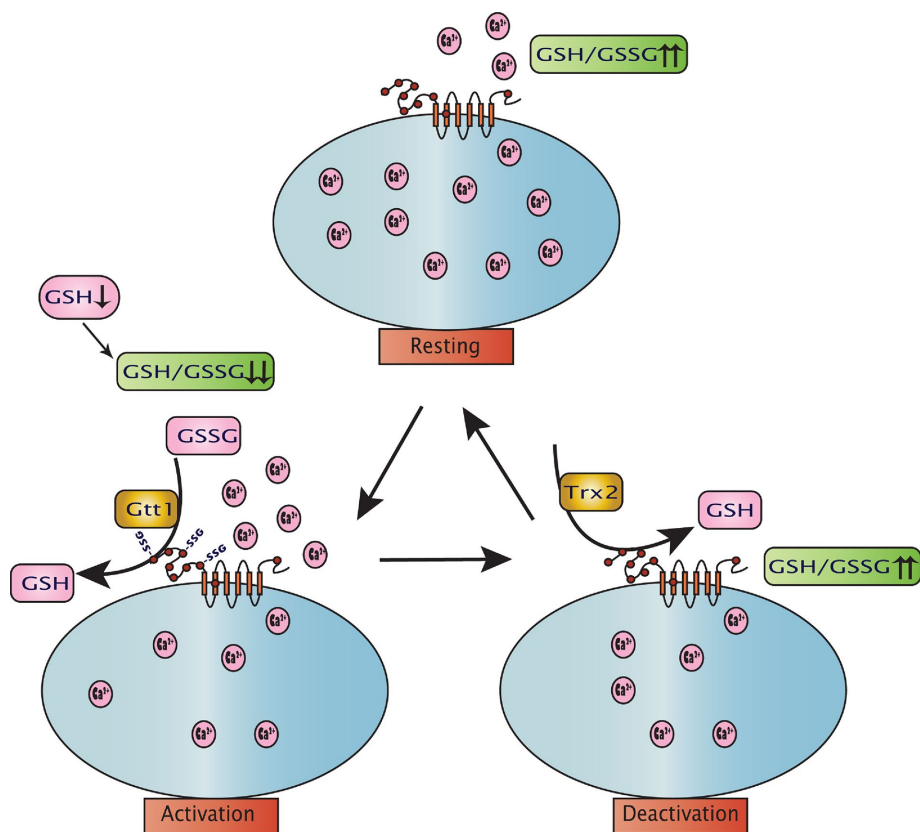


**FIGURE 9:** Model of the mechanism of YVC1 activation and restoration. Yvc1p is a vacuolar calcium release channel with its N-terminal region toward cytoplasm. Glutathione depletion in the cell changes the redox state of the glutathione toward a more oxidizing state, which leads to enzyme (Gtt1p)-dependent glutathionylation and activation of YVC1. Further, the removal of glutathione groups, that is, deglutathionylation by the enzyme Trx2p, can reverse this process, resulting in the restoration of the channel's resting state and glutathione redox balance in the cell.

study of glutathionylation of yeast proteins, the two thioredoxins were suggested to play the principal role in deglutathionylation (Greetham *et al.*, 2010), suggesting that, in the case of yeast, not only Yvc1p but possibly other proteins might also be the targets of deglutathionylation by these enzymes. In the case of YVC1, therefore, the enzyme activity of Trx2p serves to bring Yvc1p back to its resting state, which also helps in releasing reduced glutathione, further balancing the GSH:GSSG ratio in the cell (Figure 9).

Yvc1p is a mechanosensitive channel and responds to the mechanical force generated in response to hyperosmotic shock (Denis and Cyert, 2002; Zhou *et al.*, 2003). Although the precise mechanism of mechanostimulation of such channels is not understood, it is known that several pathways of the mechanical signaling cascade are redox sensitive (Schoenmakers *et al.*, 1995; Chatterjee and Fisher, 2014). Mechanical force generated using osmotic stress revealed that the yeast cell underwent a rapid change in its redox state. We also observed increased glutathionylation of Yvc1p in cells exposed to 0.8 M NaCl. These observations suggest that the mechanical response of Yvc1p may also depend on the redox modifications of this protein, and it will be interesting to investigate the link between osmotic stress and redox.

Although glutathione depletion in the yeast cells is already known to mimic low concentration of exogenous  $H_2O_2$  leading to ROS-mediated cell death (Madeo *et al.*, 1999), an important aspect of the experimental design in the present study was to use overexpressed ChaC1, an enzyme known to specifically degrade reduced glutathi-

one as a means of changing the redox conditions in vivo. This was in addition to using extracellular agents such as  $H_2O_2$ , which gives a far more rapid and drastic change in the redox status. ChaC1 is known to be acutely induced during stress conditions (Mungrue *et al.*, 2009), and thus mimics an in vivo condition, not an artificially induced situation. Our observations reveal that both these conditions can result in changes of the glutathione redox potential in the cell, although the rates of change are different. This altered redox leads to the glutathionylation of Yvc1p.

An important consequence of this study from the larger cellular perspective is that it enables one to understand the steps that lead a glutathione-depleted cell to undergo apoptosis. Even in the absence of any external oxidative insults, rapid intracellular depletion of glutathione, which can be mediated by ChaC1-like proteins induced under stress, can result in a rapid rise in intracellular calcium. Although we have not investigated the downstream effects of transient calcium influxes in the present study, increased calcium levels in the cytoplasm are known to perturb mitochondrial calcium, leading to the downstream effects and the execution of apoptosis (Ludovico *et al.*, 2002; Eisenberg *et al.*, 2007; Madeo *et al.*, 2009; Rimessi *et al.*, 2013). One hopes that using the simpler yeast apoptotic system, future studies would enable us to eventually dissect out these subsequent events in greater detail.

## MATERIALS AND METHODS

### Chemicals and reagents

All chemicals used in the present study were of either analytical or molecular biology grades and were obtained from commercial sources. Media components were purchased from Difco (USA). Oligonucleotides were purchased from Sigma (India) and IDT (USA). Restriction enzymes, Vent DNA polymerase, and other DNA-modifying enzymes were obtained from New England Biolabs (USA). Gel-extraction kits, plasmid miniprep columns, and the Ni-NTA agarose resin were obtained from Qiagen (Germany). Hybridization nitrocellulose membrane (filter type 0.45  $\mu\text{m}$ ) and Luminata forte Western horseradish peroxidase (HRP) substrate were obtained from Millipore (India). Anti-His mouse monoclonal antibody (27E8) and horse anti-mouse HRP-linked antibody were procured from Cell Signaling Technology (USA). Anti-GSH mouse monoclonal antibody (ab19534) was from Abcam (UK). Alexa Fluor 488-conjugated goat anti-mouse antibody was obtained from Molecular Probes (USA). Coelentrazine was purchased from Promega (USA).

### Strains, plasmids, and culture conditions

The strains used in this study are listed in the Supplemental Material. Plasmid pEVP11/AEQ (a plasmid bearing apoaequorin gene and a LEU2 marker) was used for calcium-measurement experiments. pRS313TEF, a centromeric yeast vector with a HIS3 marker, was used to clone and express YVC1 and its mutants. The strains were maintained on yeast extract, peptone, and dextrose (YPD)

medium and grown at 30°C. The yeast transformants were selected and maintained on synthetic defined (SD) minimal medium containing yeast nitrogen base, ammonium sulfate, and dextrose supplemented with the required amino acids. Yeast transformation was carried out by the lithium acetate method (Gietz *et al.*, 1995). The *Escherichia coli* strain DH5 $\alpha$  was used as a cloning host and grown at 37°C.

### Gene disruptions

Standard protocols were used for creating single and multiple gene deletions in yeast cells. The *GSH1* gene deletion was carried out using a *gsh1::LEU2* disruption cassette derived from *pUC19::gsh1 $\Delta$ :LEU2* (Lisowsky, 1993). Other deletions were carried out using the PCR-mediated gene-deletion strategy using either the *LEU2* or *HIS3* selection markers (Baudin *et al.*, 1993). Multiple disruptions were generated by using different nutritional markers.

### Apoptosis assays

The markers used previously to define apoptosis in yeast that include nuclear breakage, DNA fragmentation, and exposition of phosphatidylserine were carried out essentially as described earlier (Madeo *et al.*, 1997) and are briefly described below.

The terminal deoxynucleotidyl transferase (TUNEL) assay was performed using the in situ cell death detection kit (Roche Applied Science). In brief, yeast cells were fixed with 3.7% (vol/vol) formaldehyde for 30 min at room temperature and washed three times with phosphate-buffered saline (PBS). Cell walls were digested with 15 U/ml lyticase (Sigma) for 2 h at 28°C. Cells were incubated in permeabilization solution (0.1% (vol/vol) Triton X-100 and 0.1% (wt/wt) sodium citrate for 2 min on ice and rinsed twice with PBS. Cells were subsequently incubated with 20  $\mu$ l of TUNEL reaction mixture containing terminal deoxynucleotidyltransferase and FITC dUTP for 90 min at 37°C. Finally, cells were washed twice with PBS containing 1.2 M sorbitol buffer. Cells were then placed under a coverslip on a microscopic slide and observed under a fluorescence microscope.

Phosphatidylserine exposure at the membrane surface was detected by the Dead Cell Apoptosis Kit with Annexin V Alexa Fluor 488 and propidium iodide (PI). Briefly, yeast cells were washed and resuspended in sorbitol buffer (1.2 M sorbitol, 0.5 mM MgCl<sub>2</sub>, 35 mM potassium phosphate, pH 6.8) and incubated with 15 U/ml lyticase (Sigma) for 2 h at 28°C. Cells were then harvested and washed in binding buffer. Protoplasts were stained with Annexin V–Alexa Fluor 488 and PI for 20 min at room temperature. The cells were harvested, suspended in binding buffer, and analyzed by flow cytometry and applied to a microscopic slide and observed under a fluorescence microscope.

### YVC1 cloning, His tagging, and site-directed cysteine mutagenesis

YVC1 having a hexahistidine tag at the C-terminus was cloned downstream of the TEF promoter at the *Xba*I and *Xma*I sites of the pRS313TEF vector, resulting in plasmid pRS313TEF-YVC1-His. This construct was used as a template for creation of the different mutants of YVC1 by the splice overlap extension strategy. The primers used in this study are listed in the Supplemental Material. The PCR products were subcloned back into the pRS313TEF vector. The inserts were confirmed for the presence of the desired changes by sequencing.

### H<sub>2</sub>O<sub>2</sub> sensitivity assay for Yvc1p functionality

The yeast strains were transformed with plasmids containing either the WT or YVC1 mutants. Transformants were selected and grown in

SD minimal media plus supplements without histidine. The primary overnight culture was used to reinoculate the secondary culture and incubated until OD<sub>600nm</sub> = 0.6–1.5. Equal numbers of cells were harvested, washed with water, and suspended in fresh SD medium to OD<sub>600nm</sub> = 1. These cells were exposed to different concentrations ranging from 1 to 4  $\mu$ M of H<sub>2</sub>O<sub>2</sub> for 1 h. Cells were then washed, serial dilutions were prepared, and 10  $\mu$ l of each dilution was spotted on to the SD medium. The plates were incubated at 30°C for 2–3 d, after which photographs were taken.

### Protein purification and Western blot analysis

Cells exposed to extracellular agents H<sub>2</sub>O<sub>2</sub> (1.5 mM for 20 min) or diamide (1 mM for 20 min) were harvested by centrifugation at 5000 rpm for 5 min and washed subsequently with ice-cold water. The cell pellet was resuspended in 1 ml of homogenization buffer (50 mM Tris, pH 7.4, 400 mM NaCl, 10% glycerol [vol/vol], 1% Triton-X, 1 mM phenylmethylsulfonyl fluoride [PMSF], and protease inhibitor mixture [Complete, ethylenediaminetetraacetic acid-free; Roche]). Glass beads (425–600  $\mu$ m diameter) were added, and cells were lysed in a bead-beater by shaking 10 times for 1 min under the ice with a 1 min rest between shakings. Samples were centrifuged at 13,000 rpm for 20 min, and the supernatant was incubated with 500  $\mu$ l Ni-NTA agarose (Qiagen) at 4°C for 2–3 h. Samples were cooled for 10 min on the ice before centrifugation at 1000 rpm for 1 min. Pellets were resuspended gently in 10 ml ice-cold wash buffer (50 mM Tris, pH 7.4, 10% [vol/vol] glycerol, 300 mM NaCl, 30 mM imidazole, pH 6.5, 1.5 mM PMSF), and the centrifugation was repeated. Two more washing steps were carried out with wash buffer. The slurry was resuspended in 200  $\mu$ l of elution buffer (50 mM Tris, pH 7.4, 10% [vol/vol] glycerol, 0.3 M imidazole, pH 6.5, 1.5 mM PMSF) and incubated at 4°C with gentle shaking for 5 min. Finally, the slurry was centrifuged at 1000 rpm for 5 min, and the eluted protein supernatant was collected. Protein content was estimated by the Bradford method. Immunoblot analysis of Ni-NTA-purified wild type Yvc1p and its mutants was done as described earlier. Equal amounts of protein samples denatured in protein sample buffer (100 mM Tris-HCl, pH 8, 4% [wt/vol] SDS, 5 mM EDTA, 40% [vol/vol] glycerol, and 0.05% [vol/vol] bromophenol blue) at 40°C for 10 min were resolved by nonreducing SDS/PAGE (10% acrylamide gel), electroblotted onto nitrocellulose membrane, and probed with mouse monoclonal anti-His and anti-GSH primary antibody at a dilution of 1:3000. The proteins were finally probed with goat anti-mouse HRP-conjugated secondary immunoglobulin G (IgG) and visualized using chemiluminescence detection reagent. For in vitro glutathionylation, purified YVC1 was incubated with 1 mM GSH and 0.5 mM diamide. Purified protein was incubated with 10 mM IAM and NEM (1 h at pH 7.5) for cysteine alkylation. To quantify the protein expression levels, we used Image J software for the densitometry analysis of the band signals. The resulting signal intensity was normalized with respect to the band surface area and expressed as percentage expression levels compared with control Yvc1p (anti-His).

### Cellular localization of the YVC1 and cysteine mutants

For determining the localization of Yvc1p and its cysteine mutants, an indirect immunofluorescence protocol for budding yeast was followed (Kilmartin and Adams, 1984). Exponentially growing cultures were fixed for 2 h with 4% formaldehyde in 0.1 M potassium phosphate (pH 7.4). Cells were spheroplasted and permeabilized with 0.4% Triton-X before being stained with rabbit monoclonal anti-His and mouse monoclonal antibody against the vacuolar marker protein ATP6V1A (Abcam ab113745). Primary antibody staining was

detected with anti-rabbit Alexa Fluor 647 and anti-mouse Alexa Fluor 488-conjugated secondary antibodies (Molecular Probes). Images were visualized for fluorescence and Nomarski optics using a Zeiss microscope with a 64× oil objective and photographed using an AxioCam MRc5 camera.

### Determination of intracellular Ca<sup>2+</sup> levels

Cytosolic Ca<sup>2+</sup> concentration was determined using the apoaequorin expression system (Nakajima-Shimada *et al.*, 1991). Yeast strains were transformed with the plasmid pEVP11/AEQ containing the apoaequorin gene, and transformants were selected for growth on SD medium lacking leucine. For luminescence assays, cells were grown overnight at 30°C in SD-Leu medium and harvested during exponential growth. These cells were resuspended at a density of ~10<sup>8</sup> cells/ml in fresh SD-Leu medium. To reconstitute functional aequorin, 5 μM coelenterazine (stock solution 1 mM dissolved in methanol) was added, and cells were incubated for 5 h at 30°C in the dark. Cells were collected by centrifuging at 5000 rpm for 5 min, washed three times, resuspended in 200 μl of medium, and incubated for 30 min in order to reconstitute functional aequorin within the cells. After incubation, cells were transferred to a 96-well microplate. The baseline luminescence was recorded for 10 min, and after addition of H<sub>2</sub>O<sub>2</sub>, the light emission was monitored for 60 min. For experiments involving calcium changes due to intracellular glutathione depletion, the luminescence was recorded for 250 min. For determining Yvc1p-dependent calcium flux, EGTA was added to the cell suspension at a final concentration of 5 mM at 10 min before application of stress to avoid the interference of calcium flux from plasma membrane calcium channels. The light emission is reported as relative luminescence units (RLUs) over time using a similar number of cells per sample. Because light units cannot be accurately converted into intracellular Ca<sup>2+</sup> concentrations, our results are presented as relative quantities. Cell lysis with 0.4% Triton-X plus 10 mM CaCl<sub>2</sub> allowed confirmation that all measurements had been done in non-limiting conditions for aequorin. Multiple determinations were performed for each condition.

### Statistical analysis

In the Western blot quantification, *p* values were generated by analysis of variance. Multiple comparisons were corrected by the Bonferroni *t* test (\*, *p* < 0.05; \*\*, *p* < 0.01; \*\*\*, *p* < 0.001; *n* ≥ 3 assays) in Prism 4 (GraphPad). All error bars represent mean ± SD based on three independent experiments. In the fluorescence experiments, statistical analyses were performed using a paired Student's *t* test.

### ACKNOWLEDGMENTS

We thank Patrick Masson, University of Wisconsin–Madison, for the pEVP11/AEQ plasmid. We also thank Muskan Bhatia, IISER Mohali, for help in some experiments and for critical suggestions. A.C. is the recipient of a senior research fellowship from the Council of Scientific and Industrial Research, India. K.K.D. acknowledges support from Department of Science and Technology INSPIRE, A.K.B. is a recipient of the JC Bose National Fellowship from the Department of Science and Technology. The study was supported by a Grant-in-Aid (project no. SB/SO/BB-017/2014) from the Department of Science and Technology, Government of India.

### REFERENCES

Bandell M, Story GM, Hwang SW, Viswanath V, Eid SR, Petrus MJ, Earley TJ, Patapoutian A (2004). Noxious cold ion channel TRPA1 is activated by pungent compounds and bradykinin. *Neuron* 41, 849–857.

Barreto L, Garcerá A, Jansson K, Sunnerhagen P, Herrero E (2006). A peroxisomal glutathione transferase of *Saccharomyces cerevisiae* is functionally related to sulfur amino acid metabolism. *Eukaryot Cell* 5, 1748–1759.

Baudin A, Ozier-Kalogeropoulos O, Denouel A, Lacroute F, Cullin C (1993). A simple and efficient method for direct gene deletion in *Saccharomyces cerevisiae*. *Nucleic Acids Res* 21, 3329–3330.

Bootman MD, Lipp P, Berridge MJ (2001). The organisation and functions of local Ca<sup>2+</sup> signals. *J Cell Sci* 114, 2213–2222.

Brookes PS, Yoon Y, Robotham JL, Anders MW, Sheu S-S (2004). Calcium, ATP, and ROS: a mitochondrial love-hate triangle. *Am J Physiol Cell Physiol* 287, C817–C833.

Carmona-Gutierrez D, Eisenberg T, Büttner S, Meisinger C, Kroemer G, Madeo F (2010). Apoptosis in yeast: triggers, pathways, subroutines. *Cell Death Differ* 17, 763–773.

Chatterjee S, Fisher AB (2014). Mechanotransduction: forces, sensors, and redox signaling. *Antioxid Redox Signal* 20, 868–871.

Chekmeneva E, Prohens R, Díaz-Cruz JM, Ariño C, Esteban M (2008). Thermodynamics of Cd<sup>2+</sup> and Zn<sup>2+</sup> binding by the phytochelatin (γ-Glu-Cys)<sub>4</sub>-Gly and its precursor glutathione. *Anal Biochem* 375, 82–89.

Choi JH, Lou W, Vancura A (1998). A novel membrane-bound glutathione S-transferase functions in the stationary phase of the yeast *Saccharomyces cerevisiae*. *J Biol Chem* 273, 29915–29922.

Clapham DE (2003). TRP channels as cellular sensors. *Nature* 426, 517–524.

Clapham DE (2007). Calcium signaling. *Cell* 131, 1047–1058.

Clapham DE, Julius D, Montell C, Schultz G (2005). International Union of Pharmacology. XLIX. nomenclature and structure-function relationships of transient receptor potential channels. *Pharmacol Rev* 57, 427–450.

Collinson EJ, Grant CM (2003). Role of yeast glutaredoxins as glutathione S-transferases. *J Biol Chem* 278, 22492–22497.

Cui J, Kaandorp JA, Ositelu OO, Beaudry V, Knight A, Nanfack YF, Cunningham KW (2009a). Simulating calcium influx and free calcium concentrations in yeast. *Cell Calcium* 45, 123–132.

Cui J, Kaandorp JA, Sloot PMA, Lloyd CM, Filatov MV (2009b). Calcium homeostasis and signaling in yeast cells and cardiac myocytes. *FEMS Yeast Res* 9, 1137–1147.

Cunningham KW (2011). Acidic calcium stores of *Saccharomyces cerevisiae*. *Cell Calcium* 50, 129–138.

Denis V, Cyert MS (2002). Internal Ca<sup>2+</sup> release in yeast is triggered by hypertonic shock and mediated by a TRP channel homologue. *J Cell Biol* 156, 29–34.

Dunn T, Gable K, Beeler T (1994). Regulation of cellular Ca<sup>2+</sup> by yeast vacuoles. *J Biol Chem* 269, 7273–7278.

Eisenberg T, Büttner S, Kroemer G, Madeo F (2007). The mitochondrial pathway in yeast apoptosis. *Apoptosis Int J Program Cell Death* 12, 1011–1023.

Ermak G, Davies KJA (2002). Calcium and oxidative stress: from cell signaling to cell death. *Mol Immunol* 38, 713–721.

Findlay VJ, Townsend DM, Morris TE, Fraser JP, He L, Tew KD (2006). A novel role for human sulfiredoxin in the reversal of glutathionylation. *Cancer Res* 66, 6800–6806.

Franco R, Cidlowski JA (2009). Apoptosis and glutathione: beyond an antioxidant. *Cell Death Differ* 16, 1303–1314.

Franco R, DeHaven WI, Sifre MI, Bortner CD, Cidlowski JA (2008). Glutathione depletion and disruption of intracellular ionic homeostasis regulate lymphoid cell apoptosis. *J Biol Chem* 283, 36071–36087.

Gietz RD, Schiestl RH, Willems AR, Woods RA (1995). Studies on the transformation of intact yeast cells by the LiAc/SS-DNA/PEG procedure. *Yeast* 11, 355–360.

Gilbert HF (1990). Molecular and cellular aspects of thiol-disulfide exchange. *Adv Enzymol Relat Areas Mol Biol* 63, 69–172.

Giorgi C, Romagnoli A, Pinton P, Rizzuto R (2008). Ca<sup>2+</sup> signaling, mitochondria and cell death. *Curr Mol Med* 8, 119–130.

Greetham D, Vickerstaff J, Shenton D, Perrone GG, Dawes IW, Grant CM (2010). Thioredoxins function as deglutathionylase enzymes in the yeast *Saccharomyces cerevisiae*. *BMC Biochem* 11, 3.

Grek CL, Zhang J, Manevich Y, Townsend DM, Tew KD (2013). Causes and consequences of cysteine S-glutathionylation. *J Biol Chem* 288, 26497–26504.

Gutscher M, Pauleau A-L, Marty L, Brach T, Wabnitz GH, Samstag Y, Meyer AJ, Dick TP (2008). Real-time imaging of the intracellular glutathione redox potential. *Nat Methods* 5, 553–559.

Han YH, Kim SH, Kim SZ, Park WH (2008). Apoptosis in arsenic trioxide-treated Calu-6 lung cells is correlated with the depletion of GSH levels rather than the changes of ROS levels. *J Cell Biochem* 104, 862–878.

- Hayano T, Inaka K, Otsu M, Taniyama Y, Miki K, Matsushima M, Kikuchi M (1993). PDI and glutathione-mediated reduction of the glutathionylated variant of human lysozyme. *FEBS Lett* 328, 203–208.
- Hong C, Seo H, Kwak M, Jeon J, Jang J, Jeong EM, Myeong J, Hwang YJ, Ha K, Kang MJ, et al. (2015). Increased TRPC5 glutathionylation contributes to striatal neuron loss in Huntington's disease. *Brain J Neurol* 138, 3030–3047.
- Jordt S-E, Bautista DM, Chuang H-H, McKemy DD, Zygmunt PM, Högestätt ED, Meng ID, Julius D (2004). Mustard oils and cannabinoids excite sensory nerve fibres through the TRP channel ANKTM1. *Nature* 427, 260–265.
- Jung CH, Thomas JA (1996). S-glutathiolated hepatocyte proteins and insulin disulfides as substrates for reduction by glutaredoxin, thioredoxin, protein disulfide isomerase, and glutathione. *Arch Biochem Biophys* 335, 61–72.
- Kilmartin JV, Adams AE (1984). Structural rearrangements of tubulin and actin during the cell cycle of the yeast *Saccharomyces*. *J Cell Biol* 98, 922–933.
- Kumar A, Tikoo S, Maity S, Sengupta S, Sengupta S, Kaur A, Kumar Bachhawat A (2012). Mammalian proapoptotic factor ChaC1 and its homologues function as  $\gamma$ -glutamyl cyclotransferases acting specifically on glutathione. *EMBO Rep* 13, 1095–1101.
- Li X, Qian J, Wang C, Zheng K, Ye L, Fu Y, Han N, Bian H, Pan J, Wang J, Zhu M (2011). Regulating cytoplasmic calcium homeostasis can reduce aluminum toxicity in yeast. *PLoS One* 6, e21148.
- Lisowsky T (1993). A high copy number of yeast gamma-glutamylcysteine synthetase suppresses a nuclear mutation affecting mitochondrial translation. *Curr Genet* 23, 408–413.
- Ludovico P, Rodrigues F, Almeida A, Silva MT, Barrientos A, Côte-Real M (2002). Cytochrome c release and mitochondria involvement in programmed cell death induced by acetic acid in *Saccharomyces cerevisiae*. *Mol Biol Cell* 13, 2598–2606.
- Luikenhuis S, Perrone G, Dawes IW, Grant CM (1998). The yeast *Saccharomyces cerevisiae* contains two glutaredoxin genes that are required for protection against reactive oxygen species. *Mol Biol Cell* 9, 1081–1091.
- Macpherson LJ, Dubin AE, Evans MJ, Marr F, Schultz PG, Cravatt BF, Patapoutian A (2007). Noxious compounds activate TRPA1 ion channels through covalent modification of cysteines. *Nature* 445, 541–545.
- Macpherson LJ, Geierstanger BH, Viswanath V, Bandell M, Eid SR, Hwang S, Patapoutian A (2005). The pungency of garlic: activation of TRPA1 and TRPV1 in response to allicin. *Curr Biol CB* 15, 929–934.
- Madeo F, Durchschlag M, Kepp O, Panaretakis T, Zitvogel L, Fröhlich K-U, Kroemer G (2009). Phylogenetic conservation of the preapoptotic calreticulin exposure pathway from yeast to mammals. *Cell Cycle Georget Tex* 8, 639–642.
- Madeo F, Fröhlich E, Fröhlich KU (1997). A yeast mutant showing diagnostic markers of early and late apoptosis. *J Cell Biol* 139, 729–734.
- Madeo F, Fröhlich E, Ligr M, Grey M, Sigrist SJ, Wolf DH, Fröhlich KU (1999). Oxygen stress: a regulator of apoptosis in yeast. *J Cell Biol* 145, 757–767.
- Mailloux RJ, Jin X, Willmore WG (2014). Redox regulation of mitochondrial function with emphasis on cysteine oxidation reactions. *Redox Biol* 2, 123–139.
- Manevich Y, Feinstein SI, Fisher AB (2004). Activation of the antioxidant enzyme 1-CYS peroxiredoxin requires glutathionylation mediated by heterodimerization with pi GST. *Proc Natl Acad Sci USA* 101, 3780–3785.
- Matsumoto TK, Ellsmore AJ, Cessna SG, Low PS, Pardo JM, Bressan RA, Hasegawa PM (2002). An osmotically induced cytosolic Ca<sup>2+</sup> transient activates calcineurin signaling to mediate ion homeostasis and salt tolerance of *Saccharomyces cerevisiae*. *J Biol Chem* 277, 33075–33080.
- Menon D, Board PG (2013). A role for glutathione transferase omega 1 (GSTO1-1) in the glutathionylation cycle. *J Biol Chem* 288, 25769–25779.
- Mungrue IN, Pagnon J, Kohannim O, Gargalovic PS, Lusic AJ (2009). CHAC1/MGC4504 is a novel proapoptotic component of the unfolded protein response, downstream of the ATF4-ATF3-CHOP cascade. *J Immunol* 182, 466–476.
- Nakajima-Shimada J, Iida H, Tsuji FI, Anraku Y (1991). Monitoring of intracellular calcium in *Saccharomyces cerevisiae* with an apoaequorin cDNA expression system. *Proc Natl Acad Sci USA* 88, 6878–6882.
- Ogawa N, Kurokawa T, Fujiwara K, Polat OK, Badr H, Takahashi N, Mori Y (2016). Functional and structural divergence in human TRPV1 channel subunits by oxidative cysteine modification. *J Biol Chem* 291, 4197–4210.
- Orrenius S, Zhivotovsky B, Nicotera P (2003). Regulation of cell death: the calcium-apoptosis link. *Nat Rev Mol Cell Biol* 4, 552–565.
- Palmer CP, Zhou XL, Lin J, Loukin SH, Kung C, Saimi Y (2001). A TRP homolog in *Saccharomyces cerevisiae* forms an intracellular Ca<sup>2+</sup>-permeable channel in the yeast vacuolar membrane. *Proc Natl Acad Sci USA* 98, 7801–7805.
- Popa C-V, Dumitru I, Ruta LL, Danet AF, Farcasanu IC (2010). Exogenous oxidative stress induces Ca<sup>2+</sup> release in the yeast *Saccharomyces cerevisiae*. *FEBS J* 277, 4027–4038.
- Puigpinós J, Casas C, Herrero E (2015). Altered intracellular calcium homeostasis and endoplasmic reticulum redox state in *Saccharomyces cerevisiae* cells lacking Grx6 glutaredoxin. *Mol Biol Cell* 26, 104–116.
- Rimessi A, Bonora M, Marchi S, Patergnani S, Marobbio CMT, Lasorsa FM, Pinton P (2013). Perturbed mitochondrial Ca<sup>2+</sup> signals as causes or consequences of mitophagy induction. *Autophagy* 9, 1677–1686.
- Salazar H, Llorente I, Jara-Oseguera A, García-Villegas R, Munari M, Gordon SE, Islas LD, Rosenbaum T (2008). A single N-terminal cysteine in TRPV1 determines activation by pungent compounds from onion and garlic. *Nat Neurosci* 11, 255–261.
- Schoenmakers TJ, Vaudry H, Cazin L (1995). Osmo- and mechanosensitivity of the transient outward K<sup>+</sup> current in a mammalian neuronal cell line. *J Physiol* 489, 419–430.
- Sharma KG, Sharma V, Bourbonloux A, Delrot S, Bachhawat AK (2000). Glutathione depletion leads to delayed growth stasis in *Saccharomyces cerevisiae*: evidence of a partially overlapping role for thioredoxin. *Curr Genet* 38, 71–77.
- Starke DW, Chock PB, Mieyal JJ (2003). Glutathione-thiyl radical scavenging and transferase properties of human glutaredoxin (thioltransferase). Potential role in redox signal transduction. *J Biol Chem* 278, 14607–14613.
- Tajeddine N (2016). How do reactive oxygen species and calcium trigger mitochondrial membrane permeabilisation? *Biochim Biophys Acta BBA Gen Subj* 1860, 1079–1088.
- Townsend DM, Manevich Y, He L, Hutchens S, Pazoles CJ, Tew KD (2009). Novel role for glutathione S-transferase pi. Regulator of protein S-glutathionylation following oxidative and nitrosative stress. *J Biol Chem* 284, 436–445.
- Tsunoda S, Avezov E, Zyryanova A, Konno T, Mendes-Silva L, Melo EP, Harding HP, Ron D (2014). Intact protein folding in the glutathione-depleted endoplasmic reticulum implicates alternative protein thiol reductants. *eLife* 3, e03421.
- Weinberger M, Ramachandran L, Burhans WC (2003). Apoptosis in yeasts. *IUBMB Life* 55, 467–472.
- Yoshida T, Inoue R, Morii T, Takahashi N, Yamamoto S, Hara Y, Tominaga M, Shimizu S, Sato Y, Mori Y (2006). Nitric oxide activates TRP channels by cysteine S-nitrosylation. *Nat Chem Biol* 2, 596–607.
- Yoshimoto H, Saltsman K, Gasch AP, Li HX, Ogawa N, Botstein D, Brown PO, Cyert MS (2002). Genome-wide analysis of gene expression regulated by the calcineurin/Crz1p signaling pathway in *Saccharomyces cerevisiae*. *J Biol Chem* 277, 31079–31088.
- Zhou X-L, Batiza AF, Loukin SH, Palmer CP, Kung C, Saimi Y (2003). The transient receptor potential channel on the yeast vacuole is mechanosensitive. *Proc Natl Acad Sci USA* 100, 7105–7110.